



# The role of the angiography-derived index of microcirculatory resistance in the prognosis of patients with dilated cardiomyopathy

Menghuan Li<sup>1#</sup>, Hu Su<sup>1#</sup>, Zhi Zuo<sup>1#</sup>, Zhiyong Zhang<sup>2</sup>, Mengna Li<sup>3</sup>, Fen Su<sup>4</sup>, Wenming Yao<sup>1</sup>, Yuan He<sup>1</sup>, Xiangqing Kong<sup>1,5</sup>, Hui Wang<sup>1^</sup>

<sup>1</sup>Department of Cardiology, the First Affiliated Hospital of Nanjing Medical University, Nanjing, China; <sup>2</sup>Department of Cardiology, Suqian First People's Hospital of Suqian City, Suqian, China; <sup>3</sup>Emergency Department, the First Affiliated Hospital of Nanchang University, Nanchang, China; <sup>4</sup>Outpatient Department, The First Affiliated Hospital of the University of Science and Technology of China North Campus, Hefei, China; <sup>5</sup>Gusu School, Nanjing Medical University, Suzhou, China

*Contributions:* (I) Conception and design: Menghuan Li; (II) Administrative support: H Wang, X Kong; (III) Provision of study materials or patients: Menghuan Li, H Su, Z Zuo, Mengna Li, F Su; (IV) Collection and assembly of data: H Su, Z Zhang; (V) Data analysis and interpretation: W Yao, Y He; (VI) Manuscript writing: All authors; (VII) Final approval of manuscript: All authors.

<sup>#</sup>These authors contributed equally to this work.

*Correspondence to:* Hui Wang. Department of Cardiology, the First Affiliated Hospital of Nanjing Medical University, No. 300 Guangzhou Road, Nanjing 210021, China. Email: Wangnuo@188.com; Xiangqing Kong. Department of Cardiology, the First Affiliated Hospital of Nanjing Medical University, Nanjing, China; Gusu School, Nanjing Medical University, Suzhou, China. Email: kongxq@njmu.edu.cn.

**Background:** The coronary angiography-derived index of microcirculatory resistance (caIMR) is a novel noninvasive method to assess coronary microvascular dysfunction (CMD). However, the association between caIMR and the prognosis of patients with dilated cardiomyopathy (DCM) is unclear. We aimed to explore the role of the caIMR in evaluating the outcome of patients with DCM.

**Methods:** We consecutively and retrospectively enrolled patients with DCM in the Department of Cardiology, the First Affiliated Hospital of Nanjing Medical University, Nanjing, China, from January 2013 to January 2018. The caIMR was calculated for eligible patients. The primary end point in this study was composite events, including rehospitalization related to heart failure (HF), device implantation, heart transplantation, or cardiac death. Patients were categorized into groups based on whether they had composite events (the events and no-events groups), and differences in the baseline and end points between these two groups were analyzed.

**Results:** A total of 95 eligible patients with DCM were enrolled in the study, 36 of whom had end point events. The best cutoff values of the caIMR for the left anterior descending (LAD) artery, left circumflex (LCX) artery, and right coronary artery (RCA) were >29.8 with an area under the curve (AUC) of 0.828, >25.5 with an AUC of 0.720, and >29.7 with an AUC of 0.717, respectively (all P values <0.001). Patients were then classified into the higher caIMR group and the lower caIMR group based on the cutoff value. Kaplan-Meier analyses showed that patients with a higher caIMR had increased cumulative risks of end point events regardless of the cutoff values for the LAD, LCX, and RCA (all log-rank P values <0.001). After adjustment for confounders, Cox regression analyses indicated that LAD-caIMR was an independent risk factor for end point events in patients with DCM [hazard ratio (HR) =1.11; 95% CI: 1.06–1.16].

**Conclusions:** A higher caIMR was significantly associated with the poor prognosis of patients with DCM.

<sup>^</sup> ORCID: 0000-0002-5028-9290.

**Keywords:** Dilated cardiomyopathy (DCM); index of microcirculatory resistance; coronary microvascular dysfunction (CMD); prognosis

Submitted Oct 02, 2022. Accepted for publication Feb 20, 2023. Published online Mar 15, 2023.

doi: 10.21037/qims-22-1060

View this article at: <https://dx.doi.org/10.21037/qims-22-1060>

## Introduction

Dilated cardiomyopathy (DCM), which is the third most common cause of heart failure (HF) after coronary artery disease (CAD) and hypertension, is the most frequent form of primary myocardial disease. DCM is characterized by ventricular dilation and systolic dysfunction induced by diverse genetic and non-genetic causes (1). DCM is linked to poor prognosis, and heart transplantation is often required (2). In clinical practice, patients with HF and cardiac enlargement tend to be diagnosed with DCM when other possible etiologies are excluded (e.g., CAD, hypertension, and valve diseases). Coronary angiography is the first choice to identify ischemic heart disease in the diagnostic work-up for the etiology assessment of DCM. Nevertheless, coronary angiography can only determine the ischemic myocardium caused by epicardial coronary artery stenosis, and investigation of microvascular disease is lacking in patients with DCM.

A few studies have demonstrated the presence of coronary microvascular dysfunction (CMD) in patients with DCM (3-7). The degree of CMD also has a direct impact on the prognosis of the patient (3-5). Although several techniques provide superior conditions for assessing CMD, their limitations cannot be ignored. Coronary flow reserve (CFVR) assessed using transthoracic doppler echocardiography (TTDE) is typically restricted to the left anterior descending (LAD) artery area, and cardiovascular risks are also elevated with the use of the stress dobutamine examination (3,8,9). Limited availability, associated costs, and lengthy procedure restrict the use of positron emission tomography (PET) and cardiac magnetic resonance (CMR) to evaluate myocardial blood flow (MBF) in routine clinical practice (10).

The index of microvascular resistance (IMR), which is defined as the minimum microcirculatory resistance to peak blood flow through the target vessel, is a quantitative and reproducible measure of CMD. In obtaining this index, the operator simultaneously measures the distal intracoronary pressure (Pd) and the mean conduction time

(T<sub>mn</sub>) of the intracoronary projectile saline injection by means of a pressure guidewire in a state of maximal filling of the myocardial microcirculation. The IMR value is then obtained by multiplying Pd by T<sub>mn</sub>. Adverse events in patients with stable CAD can be predicted with IMR (11,12). However, due to this approaches' complexity, time-consuming operation, and need for decongestant drugs, a coronary angiography-derived index of microcirculatory resistance (caIMR) has been proposed for the physiological evaluation of CMD. caIMR correlates well with traditional wire-based IMR and can achieve an 85% accuracy in diagnosis (13,14). For patients with ST-segment elevated myocardial infarction in the acute postoperative period, caIMR was shown to be consistent with CMR in assessing microvascular dysfunction (15).

We speculated that caIMR is associated with the outcome of the patients with DCM. Therefore, this diagnostic study was conducted to assess the role of the caIMR in the prognosis of patients with DCM. We present the following article in accordance with the STARD reporting checklist (available at <https://qims.amegroups.com/article/view/10.21037/qims-22-1060/rc>).

## Methods

### Study population

This retrospective and diagnostic study enrolled all consecutive patients with DCM in the Department of Cardiology, the First Affiliated Hospital of Nanjing Medical University, Nanjing, China, from January 2013 to January 2018. The inclusion criteria of patients in this study were as follows: (I) clinical evidence of congestion; (II) an elevated level of B-type natriuretic peptide (BNP  $\geq 35$  pg/mL) or N-terminal prohormone of B-type natriuretic peptide (NT-proBNP  $\geq 125$  pg/mL) (16); (III) echocardiographic left ventricular diameter of diastole (LVDd)  $>55$  mm for males and LVDd  $>50$  mm for females; (IV) reduced left ventricular systolic function defined by left ventricular ejection fraction (LVEF)  $<45\%$  (17),

and (V) normal or near normal coronary artery (<30% diameter stenosis) confirmed by coronary angiography. The exclusion criteria of patients were as follows: (I) a poor coronary angiogram that affected the caIMR calculation, including a blurry coronary angiography image, coronary arteries in fewer than two angiographic positions, or twisted and overlapped coronary arteries; and (II) coronary heart disease, hypertensive heart disease, rheumatic heart valve disease, myocarditis, etc.

The present study complied with the Helsinki Declaration (as revised in 2013) and was endorsed by the local institutional ethics committee of the First Affiliated Hospital of Nanjing Medical University. All patients provided written informed consent.

### *Measurement of the caIMR*

The caIMR (Rainmed Ltd., Suzhou, China) was calculated by a skilled operator who was blind to the clinical data. In order to accurately obtain the length of target vessels, two angiographic images of the target vessels with a projection angle >30° were used to rebuild a 3-dimensional vessel. Invasive aortic blood pressure was reviewed and input into the console. The caIMR was measured with FlashAngio software (Rainmed Ltd.) with a proprietary fluid dynamic algorithm that was described earlier (13). The formula of caIMR calculation was as follows:  $\text{caIMR} = \text{Pd}_{\text{hyp}} \times (\text{L}/\text{K} \times \text{V}_{\text{diastole}})$ , where  $\text{Pd}_{\text{hyp}}$  is the mean invasive blood pressure, L is the length of the target vessel measured through a 3-dimensional vessel's model,  $\text{V}_{\text{diastole}}$  is the mean coronary flow velocity assessed by the frame counts, and K is a constant (K equals 2.1). The feasibility and high accuracy of caIMR measurement are well-established (16). We also recorded the coronary angiography-derived fractional flow reserve (caFFR) from the FlashAngio system. The evaluation of caFFR was conducted as described in a previous study (18).

### *End point and follow-up*

The study end point was composite events including HF-related rehospitalization, device implantation, heart transplantation, and cardiac death during the follow-up. Criteria for HF rehospitalization were a significant elevation of BNP levels, typical dyspnea, the presence of wet rales in the lungs, decreased blood oxygen saturation (<95%), and, particularly, the use of intravenous diuretics. Device implantation included cardiac resynchronization therapy

(CRT) and CRT with a defibrillator. Patients were followed up through outpatient visits, inpatient chart reviews, and/or telephone interviews. The end point events were confirmed by reviewing medical records or contacting patients, their family members, and/or their physicians.

### *Statistical analysis*

The Kolmogorov-Smirnov test was used to determine the distribution of numerical data. Variables with a normal distribution are presented as the mean  $\pm$  standard deviation and compared using the independent samples *t*-test. Variables with skewed distribution are reported as the median with interquartile range (IQR) and were compared using the nonparametric Mann-Whitney test. Categorical variables are calculated using counts and percentages and were assessed using the chi-squared test or Fisher exact test as appropriate. For variables with a normal or nonnormal distribution, the Pearson R correlation coefficients and Spearman rank correlation coefficients were used, respectively, to analyze the correlation between the caIMR among three vessels. Based on the data collection results, the threshold of the caIMR was further explored. The receiver operating curve (ROC) analysis was used to identify the best cutoff value of the caIMR to predict the end points. Then, patients were divided into two groups according to the threshold of the caIMR. The cumulative incidence was estimated with the Kaplan-Meier method and compared between the higher caIMR and lower caIMR groups using the log-rank test. Cox proportional hazards models were adopted to calculate the hazard ratios (HRs) of the caIMR for the primary end point. The covariates in this model included age, NT-proBNP, atrial fibrillation, LVDd, the use of beta-blockers, and the use of angiotensin-converting enzyme inhibitors or angiotensin receptor blockers (ACEI/ARB). Clinical information and end point composite event results were unavailable to those conducting the experiment. A 2-sided P value <0.05 was considered statistically significant. All analyses were performed using R version 4.0.5 (The R Foundation for Statistical Computing, Vienna, Austria) and SPSS 25.0 (IBM Corp, Armonk, NY, USA).

## **Results**

*Figure 1* shows the flowchart of this study. A total of 683 patients with DCM were initially screened, and 95 patients satisfied the inclusion criteria and were finally

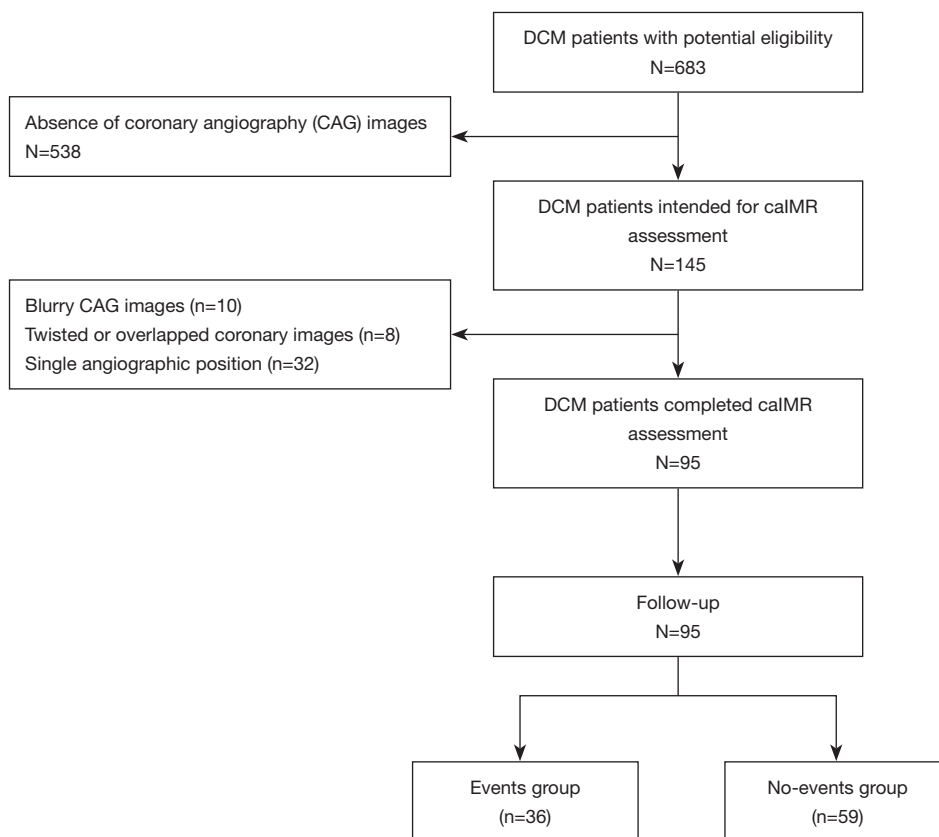


**Figure 1** A flowchart of the study. DCM, dilated cardiomyopathy; CAG, coronary angiography; caIMR, coronary angiography-derived index of microcirculatory resistance.

enrolled in this study. During a median follow-up time of 43.2 months, 36 end point events occurred. Patients were then divided into the event group and the nonevent group for comparisons of baseline characteristics.

#### **Baseline characteristics of the study population**

As shown in *Table 1*, more patients in the nonevent group used a beta-blocker (89.8% *vs.* 66.7%;  $P=0.005$ ) and ACEI/ARB (84.7% *vs.* 66.7%;  $P=0.039$ ). Patients in the event group had a higher level of LDL-C ( $2.99\pm 0.92$  *vs.*  $2.63\pm 0.65$  mmol/L;  $P=0.024$ ), caIMR of the LAD artery ( $31.6\pm 8.9$  *vs.*  $21.3\pm 5.7$ ;  $P<0.001$ ), caIMR of left circumflex (LCX) artery ( $31.9\pm 10.2$  *vs.*  $24.7\pm 10.0$ ;  $P=0.001$ ), and caIMR of right coronary artery (RCA) ( $31.8\pm 11.8$  *vs.*  $23.4\pm 7.7$ ;  $P<0.001$ ). No differences were found in age, history of disease, or echocardiographic parameters.

#### **The threshold of the caIMR in predicting the end points**

*Figure 2* shows the accuracy of the caIMR of the LAD, LCX, and RCA in predicting end points in patients with DCM. The best cutoff value of the caIMR of the LAD for end points was  $>29.8$ , with an area under the curve (AUC) of 0.828, a sensitivity of 63.9%, a specificity of 96.6%, a positive predictive value (PPV) of 92.0%, and a negative predictive value (NPV) of 81.4% (*Table 2*). The optimal predictive value of the caIMR of the LCX was  $>25.5$  with an AUC of 0.720 ( $P<0.001$ ). Additionally, the threshold of the caIMR of the RCA to determine end points was  $>29.7$  with an AUC of 0.717 ( $P<0.001$ ).

#### **Survival analysis based on the caIMR**

The median follow-up period of all patients was

**Table 1** Baseline characteristics of the events group and no-events group

Variables	Events group (n=36)	No-events group (n=59)	P value
Age (years)	64 [53, 68]	63 [50, 68]	0.890
Male, n (%)	30 (83.3)	43 (72.9)	0.241
Diabetes, n (%)	3 (8.3)	11 (18.6)	0.237
Stroke, n (%)	1 (2.8)	3 (5.1)	1.000
Atrial fibrillation, n (%)	11 (30.6)	9 (15.3)	0.076
Smoker, n (%)	25 (69.4)	29 (49.2)	0.053
SBP (mmHg)	115±17	118±16	0.345
DBP (mmHg)	74±11	70±11	0.186
NT-proBNP (pg/mL)	1,286 [766, 2,602]	1,143 [535, 2,360]	0.203
TC (mmol/L)	4.55±1.24	4.18±0.99	0.111
LDL-C (mmol/L)	2.99±0.92	2.63±0.65	0.024
FBG (mmol/L)	5.07 [4.62, 5.71]	5.27 [4.80, 5.83]	0.273
LAD (mm)	47.2±7.3	45.2±5.8	0.134
LVDs (mm)	57.9±10.0	58.0±9.3	0.952
LVDd (mm)	68.0±9.7	68.9±9.0	0.624
RAD (mm)	38.9±7.0	38.9±7.1	0.953
RVDd (mm)	40.1±8.6	37.1±8.6	0.106
LVEF (%)	32.3±7.3	33.1±7.7	0.615
Beta-blocker, n (%)	24 (66.7)	53 (89.8)	0.005
ACEI/ARB, n (%)	24 (66.7)	50 (84.7)	0.039
LAD-caIMR	31.6±8.9	21.3±5.7	<0.001
LCX-caIMR	31.9±10.2	24.7±10.0	0.001
RCA-caIMR	31.8±11.8	23.4±7.7	<0.001

Data are expressed as n (%) or median [Q1, Q3] or mean ± standard deviation. SBP, systolic blood pressure; DBP, diastolic blood pressure; NT-proBNP, N-terminal prohormone of B-type natriuretic peptide; TC, total cholesterol; LDL-C, low-density lipoprotein cholesterol; FBG, fast blood glucose; LAD, left atrial diameter; LVDs, left ventricular diameter of systole; LVDd, left ventricular diameter of the diastole; RAD, right atrial diameter; RVDd, right ventricular diameter of the diastole; LVEF, left ventricular ejection fraction; ACEI, angiotensin-converting enzyme inhibitor; ARB, angiotensin receptor blockers; LAD-caIMR, coronary angiography-derived index of microcirculatory resistance for left anterior descending artery; LCX-caIMR, coronary angiography-derived index of microcirculatory resistance for left circumflex artery; RCA-caIMR, coronary angiography-derived index of microcirculatory resistance for right coronary artery.

43.2 months, and 36 (37.9%) patients had their end point during this period. Specifically, there were 22 HF-related rehospitalizations, 6 device implantations, 1 heart transplantation, and 7 deaths. When patients were divided into the higher caIMR and lower caIMR groups according to the cutoff value of each coronary artery, Kaplan-Meier analysis showed that patients with a higher caIMR had an increased cumulative risk of an end point regardless of

the cutoff values of the LAD, LCX, and RCA (*Figure 3*; all log-rank P values <0.001). Furthermore, we evaluated the differences in each component of the end points in the higher caIMR and lower caIMR groups stratified by the 3 coronary arteries (*Figure S1*). We found that patients with a higher caIMR had a greater frequency of HF-related rehospitalization (all P values <0.001). There were no differences in device implantation, heart transplantation, or

death between the groups.

### Effect of the caIMR on the end points

The use of beta-blockers, atrial fibrillation, LAD-caIMR, LCX-caIMR, and RCA-caIMR were significantly associated with the end points of patients with DCM in the unadjusted model. After adjustment for confounders, LAD-caIMR remained significant in predicting adverse outcomes in patients with DCM, indicating that LAD-caIMR was an

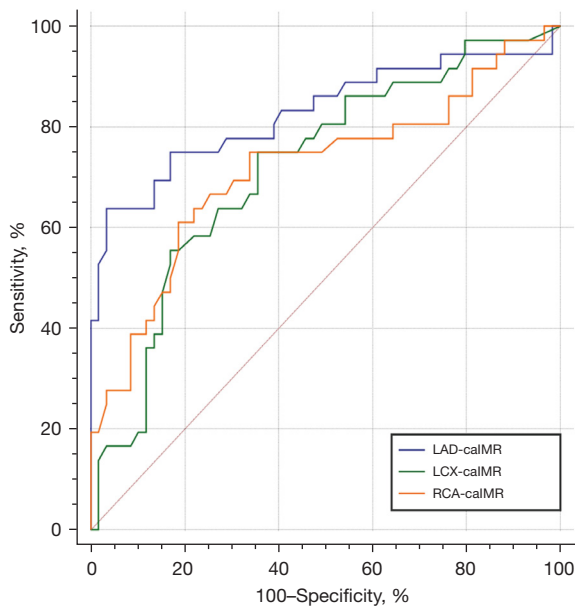


**Figure 2** ROC analyses of the caIMR for the primary end point. LAD-caIMR, coronary angiography-derived index of microcirculatory resistance for left anterior descending artery; LCX-caIMR, coronary angiography-derived index of microcirculatory resistance for left circumflex artery; RCA-caIMR, coronary angiography-derived index of microcirculatory resistance for right coronary artery; ROC, receiver operating characteristic.

independent predictor for primary end points. Each 1 unit raised in LAD-caIMR contributed to an 11% increased risk of primary end points (Table 3; HR =1.11, 95% CI: 1.06–1.16).

### Consistency of the caIMR among the LAD, LCX, and RCA regions

In order to explore the relationships between the caIMR values among the 3 coronary artery regions, we used a pie chart (Figure 4) and scatter plots (Figure 5) to compare the values of the caIMR in the three vessels. We divided the caIMR into high and low groups based on the cutoff values of each vessel from the ROC analyses. Figure 4 shows the distribution of the eight categories. The consistency with high-high-high and low-low-low accounted for 36.38% and 10.11% of total distribution of the caIMR among the three vessels, respectively. An almost 50% inconsistency of the caIMR was observed in 3 coronary artery domains. Furthermore, Figure 5 shows the correlations among the three vessels based on scatter plots. These findings showed a moderate correlation for each artery (R for LAD: 0.409; R for LCX: 0.461; R for RCA: 0.413;  $P < 0.001$ ).

## Discussion

This study is the first to assess the impact of coronary microvascular function on patients with DCM using the caIMR. The primary conclusion of our study was that caIMR could be a good predictor of adverse effects in patients with DCM. This new finding suggests that the measurement of the caIMR may provide an objective method of risk stratification for patients with DCM.

Histological examination of the hearts of patients with DCM shows unequal interstitial fibrosis, degenerated cardiomyocytes, and dilated heart chambers as the main

**Table 2** Predictive value of the caIMR for end points

Index	Positive threshold	AUC	Sen (%)	Spe (%)	PPV (%)	NPV (%)	P value
LAD-caIMR	>29.8	0.828	63.9	96.6	92.0	81.4	<0.001
LCX-caIMR	>25.5	0.720	75.0	64.4	56.3	80.8	<0.001
RCA-caIMR	>29.7	0.717	61.1	81.4	66.7	77.4	<0.001

caIMR, coronary angiography-derived index of microcirculatory resistance; LAD-caIMR, coronary angiography-derived index of microcirculatory resistance for left anterior descending artery; LCX-caIMR, coronary angiography-derived index of microcirculatory resistance for left circumflex artery; RCA-caIMR, coronary angiography-derived index of microcirculatory resistance for right coronary artery; AUC, area under the curve; Sen, sensitivity; Spe, specificity; PPV, positive predictive value; NPV, negative predictive value.

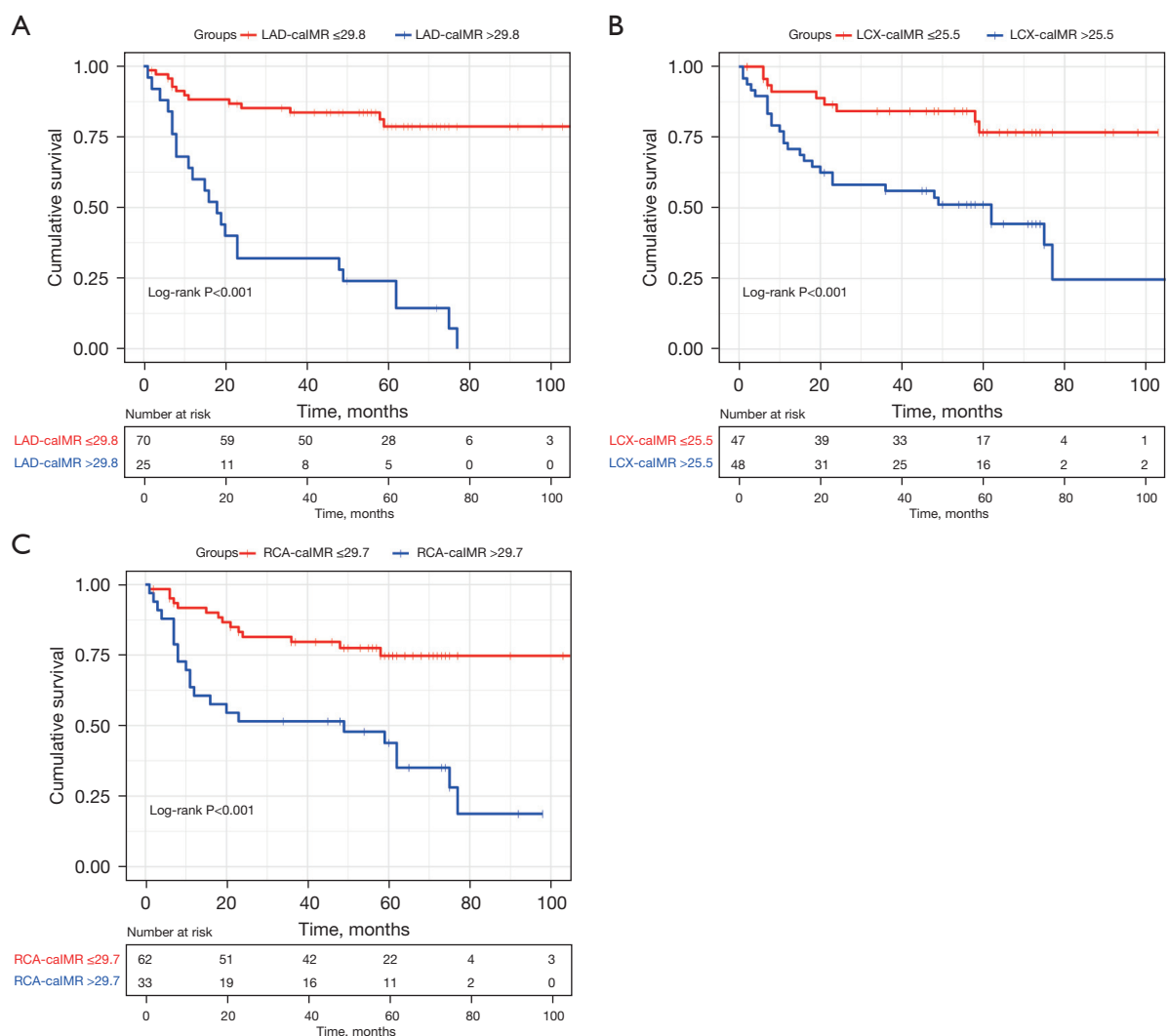


**Figure 3** Kaplan-Meier curves comparing the differences of cumulative risk of the primary end point in patients with DCM based on the caIMR. (A) Kaplan-Meier curves of patients with DCM according to the results of the LAD-caIMR. (B) Kaplan-Meier curves of patients with DCM according to the results of the LCX-caIMR. (C) Kaplan-Meier curves of patients with DCM according to the results of the RCA-caIMR. LAD-caIMR, coronary angiography-derived index of microcirculatory resistance for left anterior descending artery; LCX-caIMR, coronary angiography-derived index of microcirculatory resistance for left circumflex artery; RCA-caIMR, coronary angiography-derived index of microcirculatory resistance for right coronary artery; DCM, dilated cardiomyopathy.

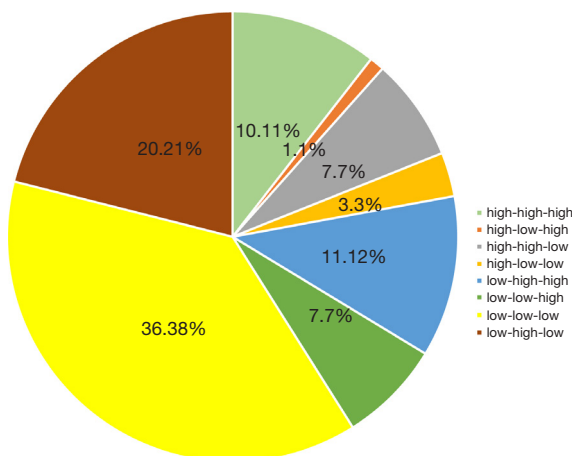
pathological disorders of this disease (19). Myocardial ischemia was not previously assumed to play a role in the progression of the disease because it contains anatomically normal epicardial coronary arteries. However, rapidly evolving microcirculation assessment techniques, such as TTDE, CMR, and PET, have provided powerful support to conflict with traditional perceptions (20,21). Previous coronary endothelial dysfunction studies have shown that vascular abnormalities are closely related to myocardial

fibrosis in patients with DCM (22). These studies indicated that DCM is also associated with vascular dysfunction for development and progression and represents a major predictor of adverse events even in the absence of CAD. However, current methods for assessing microcirculation in DCM are not suitable for large-scale clinical development. As a result, an ideal assessment method for assessing the severity of the disease and determining a worse prognosis may be useful for making treatment decisions.

**Table 3** Unadjusted and adjusted Cox regression analyses of the caIMR for outcomes in patients with DCM

Variables	Unadjusted analysis		Adjusted analysis	
	HR (95% CI)	P value	HR (95% CI)	P value
Age	1.00 (0.97–1.04)	0.744	1.01 (0.98–1.05)	0.478
NT-proBNP	1.00 (1.00–1.00)	0.142	1.00 (1.00–1.00)	0.004
AF	2.21 (1.08–4.54)	0.031	2.17 (0.96–4.96)	0.061
LVDd	0.99 (0.96–1.03)	0.710	1.04 (1.00–1.09)	0.064
Beta-blockers	0.39 (0.20–0.79)	0.008	0.52 (0.24–1.13)	0.098
ACEI/ARB	0.56 (0.28–1.12)	0.102	0.63 (0.29–1.35)	0.231
LAD-caIMR	1.11 (1.07–1.15)	<0.001	1.11 (1.06–1.16)	<0.001
LCX-caIMR	1.04 (1.01–1.06)	0.003	0.99 (0.95–1.03)	0.591
RCA-caIMR	1.05 (1.02–1.07)	0.001	1.04 (1.00–1.07)	0.053

caIMR, coronary angiography-derived index of microcirculatory resistance; DCM, dilated cardiomyopathy; NT-proBNP, N-terminal prohormone of B-type natriuretic peptide; AF, atrial fibrillation; LVDd, left ventricular diameter of the diastole; ACEI, angiotensin-converting enzyme inhibitor; ARB, angiotensin receptor blockers; LAD-caIMR, coronary angiography-derived index of microcirculatory resistance for left anterior descending artery; LCX-caIMR, coronary angiography-derived index of microcirculatory resistance for left circumflex artery; RCA-caIMR, coronary angiography-derived index of microcirculatory resistance for right coronary artery; HR, hazard ratio; CI, confidence interval.

**Figure 4** Distribution of the caIMR among the 3 vessels. caIMR, coronary angiography-derived index of microcirculatory resistance.

In addition to the above-mentioned methods, existing literature has demonstrated the convenience of IMR as a standard for identifying microvascular damage (23). However, due to the increased procedural time, procedural costs, complexity of wire-derived IMR, and other factors affecting the results, IMR has not been extensively used in clinical diagnosis and therapy (24,25). With the development of computational fluid dynamics technology,

caIMR, a type of imaging-derived functional indicator, has advanced the evaluation of CMD. It is well documented that caIMR has excellent diagnostic accuracy and consistency with CMR and traditional IMR for patients with ST-segment elevation myocardial infarction (STEMI) (13,14). Furthermore, caIMR is capable of predicting the risk of cardiac death and the readmission rate for patients with STEMI after they undergo percutaneous coronary intervention (PCI) (26,27). For myocardial infarction with non-obstructive coronary arteries (MINOCA), CMD has also been widely identified and can be detected in 30–56% of those patients treated in a catheterization laboratory (28,29). The prognostic value of the caIMR based on cutoff values also has clinical importance, with the best cutoff being >43 U (30). However, the predictive value of the caIMR in DCM is unclear. Our findings showed that the caIMR was significantly high in patients with DCM, and higher levels of LAD-caIMR (>29.8 U) were linked to lower survival rates, providing further support for the clinical importance of the caIMR in diagnosing and treating DCM.

Currently, the range of normal values for caIMR is inconclusive. As the caIMR was in good agreement with IMR, we may be able to derive the corresponding trends in the caIMR from the changes in IMR. Melikian *et al.* (31) analyzed 101 cases of epicardial coronary lesions and found that the normal value of IMR should be less than 25. The



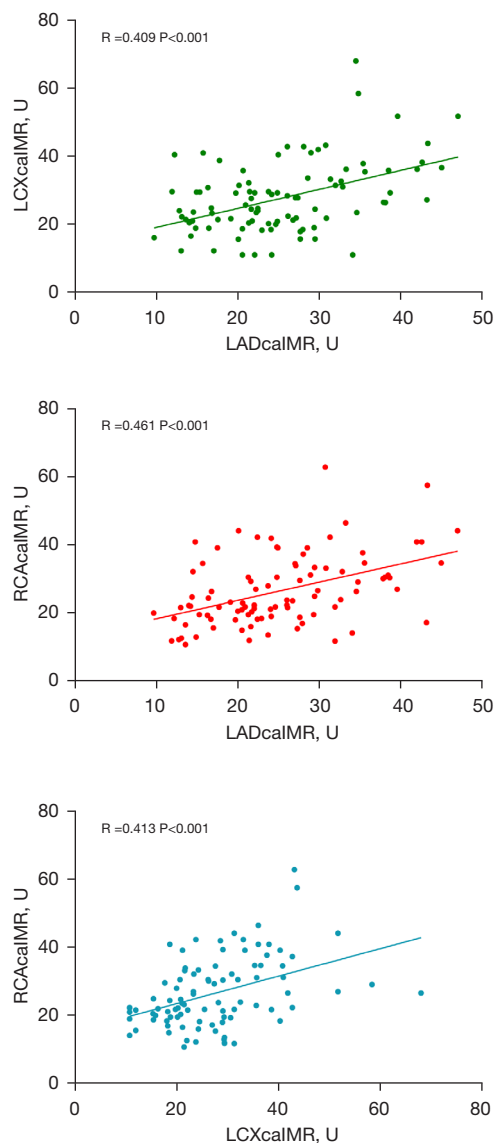


**Figure 5** Correlation of the caIMR among the 3 vessels. LAD-caIMR, coronary angiography-derived index of microcirculatory resistance for left anterior descending artery; LCX-caIMR, coronary angiography-derived index of microcirculatory resistance for left circumflex artery; RCA-caIMR, coronary angiography-derived index of microcirculatory resistance for right coronary artery.

average IMR of patients with normal coronary angiograms found in a study of Europeans was  $19 \pm 5$ , while that of a normal Chinese population reported by Luo *et al.* (32) was  $18.8 \pm 5.6$ .

Previous studies have demonstrated that the IMR of diseased vessels in patients with STEMI may be generally

greater than 40 (26,27). For patients with MINOCA, an IMR greater than 43 is a key risk stratification indicator (30). The elevated caIMR shows the presence of CMD and myocardial ischemic change. To our knowledge, ours is the first study to assess the role of the caIMR in the DCM population. LAD-caIMR  $>29.8$  was found to be an independent influencing factor of poor prognosis in our study. As for the reasons for the lower caIMR values in patients with dilated heart disease compared to those with myocardial infarction, we speculate that this may be due to poor myocardial perfusion caused by a greater number of plaque remnants and degree of thrombus dislodging into the distal microvasculature. In this study, we used offline caIMR assessments, so intracoronary nitroglycerin was not administered prior to angiography, which might be more biased compared to online caIMR. However, a study using offline caIMR to estimate the accuracy of the caIMR indicated that offline caIMR had excellent consistency with wire-based IMR, with an AUC of 0.919 (13). We surmised that the offline caIMR used in our study is capable of assessing CMD. In our study, there was a significantly higher level of low-density lipoprotein-cholesterol (LDL-C) in the event group than in the nonevent group. Atorvastatin has been reported to be effective in improving the performance of LVEF, inhibiting inflammation, and alleviating endothelium damage and endothelial dysfunction, which helps improve CMD in patients with DCM (33,34). Lovastatin was also shown to improve endothelial dysfunction and cellular cross-talk in DCM (35). We observed higher use of ACEI/ARB and beta-blockers in the no-events group, which might have been due to their positive effect on microcirculation as reported in previous studies (36,37).

ACEI/ARB beneficially influences cardiac function through mechanisms that improve CMD, including anti-inflammatory effects and anti-oxidative stress, strengthening both endothelial and microvascular function and rebalancing sympathetic dysregulation. Beta-blockers with vasodilatory effects improve the left ventricular filling pressure. Although ACEI and beta-blocker usage was lower in the events group and the protective effect of beta-blockers was confirmed with univariate regression, LAD-IMR remained strongly associated with adverse events after these variables were adjusted for, suggesting that high LAD-IMR remains an independent factor of poor prognosis in patients with DCM. Other reasons explaining the lower caIMR in patients with DCM were attributed to the lack of ischemia-reperfusion injury caused by PCI after

vessel opening, which could have led to the destruction of the microcirculation compared in contrast to myocardial infarction.

We maintain a positive outlook on the treatment of CMD in patients with DCM. In addition to the drugs and devices commonly used in clinical practice, it has been reported that transplantation of CD34 (+) stem cells can promote the formation of new blood vessels in ischemic tissue by immediately incorporating cells brought into the creating vascular system or using producing and secreting angiogenic cytokines (38,39). Inhibitors of cyclic nucleotide phosphodiesterase PDE3 with vasodilatory actions may also be considered an adjunct therapy for DCM (40). Vascular endothelial growth factor B (*VEGF-B*) gene therapy also demonstrated its intracoronary cytoprotective function in a preclinical animal model of DCM (41). Furthermore, we noticed that the corrected thrombolysis in the myocardial infarction frame count (CTFC) correlated well with the caIMR and had a strong predictive power to identify CMD (42). We look forward to the development of more precise and convenient treatment tools for patients with CMD (42).

Several limitations of this study should be noted. First, the retrospective, single-center design possibly generated bias. Second, the main rationale for using CMR is to exclude confusing diagnoses, but this approach was rarely used in our study, which might have affected the accuracy of the diagnosis of DCM. It would be intriguing to explore the relationship between myocardial fibrosis and microcirculatory disorders. CMR is a promising tool for estimating myocardial fibrosis in DCM in clinical practice (43). However, we were not able to explore the relationship between CMD and fibrosis because the study contained a limited amount of cardiac MR data. A prospective cohort study is required to trace the time sequence of the myocardial fibrosis and CMD during a long-term follow-up in DCM. Doing so could better determine whether CMD is a side-effect of fibrosis or a potential pathophysiologic link in CMD-induced DCM. Finally, the caIMR was measured using blood pressure and coronary flow at rest, which might have biased the results from the invasive wire-based IMR using adenosine at hyperemia.

## Conclusions

The caIMR was significantly associated with a poor prognosis in patients with DCM. Active assessment of the

caIMR in patients with DCM may help in improved risk stratification and targeted treatment.

## Acknowledgments

We would like to thank Rainmed Ltd., Suzhou, China, for supporting the computation of the caIMR.

*Funding:* This work was supported by the Science Foundation of Gusu School (No. GSKY20220102 to Xiangqing Kong), the Natural Science Foundation of Jiangsu Province (No. BK2012648 to Hui Wang), the Nanjing Science and Technology Innovation Projects for Overseas Graduates and the National Science Fund for Distinguished Young Scholars (No. 8220021578 to Zhi Zuo), and the General Scientific Research Project of Jiangsu Provincial Health Commission (No. M2020083 to Zhiyong Zhang).

## Footnote

*Reporting Checklist:* The authors have completed the STARD reporting checklist. Available at <https://qims.amegroups.com/article/view/10.21037/qims-22-1060/rc>

*Conflicts of Interest:* All authors have completed the ICMJE uniform disclosure form (available at <https://qims.amegroups.com/article/view/10.21037/qims-22-1060/coif>). XK received funding from the Science Foundation of Gusu School (No. GSKY20220102); HW received funding from the Natural Science Foundation of Jiangsu Province (No. BK2012648). Zhi Zuo received funding from the Nanjing Science and Technology Innovation Projects for Overseas Graduates and the National Science Fund for Distinguished Young Scholars (No. 8220021578). Zhiyong Zhang received funding from the General Scientific Research Project of Jiangsu Provincial Health Commission (No. M2020083). The other authors have no conflicts of interest to declare.

*Ethical Statement:* The authors are accountable for all aspects of the work in ensuring that questions related to the accuracy or integrity of any part of the work are appropriately investigated and resolved. The study protocol was approved by the independent institutional ethics committee of the First Affiliated Hospital of Nanjing Medical University and complied with the Declaration of Helsinki (as revised in 2013). Written informed consent was acquired from all patients.

*Open Access Statement:* This is an Open Access article distributed in accordance with the Creative Commons Attribution-NonCommercial-NoDerivs 4.0 International License (CC BY-NC-ND 4.0), which permits the non-commercial replication and distribution of the article with the strict proviso that no changes or edits are made and the original work is properly cited (including links to both the formal publication through the relevant DOI and the license). See: <https://creativecommons.org/licenses/by-nc-nd/4.0/>.

## References

- Pinto YM, Elliott PM, Arbustini E, Adler Y, Anastasakis A, Böhm M, et al. Proposal for a revised definition of dilated cardiomyopathy, hypokinetic non-dilated cardiomyopathy, and its implications for clinical practice: a position statement of the ESC working group on myocardial and pericardial diseases. *Eur Heart J* 2016;37:1850-8.
- Weintraub RG, Semsarian C, Macdonald P. Dilated cardiomyopathy. *Lancet* 2017;390:400-14.
- Rigo F, Gherardi S, Galderisi M, Pratali L, Cortigiani L, Sicari R, Picano E. The prognostic impact of coronary flow-reserve assessed by Doppler echocardiography in non-ischaemic dilated cardiomyopathy. *Eur Heart J* 2006;27:1319-23.
- Rigo F, Gherardi S, Galderisi M, Sicari R, Picano E. The independent prognostic value of contractile and coronary flow reserve determined by dipyridamole stress echocardiography in patients with idiopathic dilated cardiomyopathy. *Am J Cardiol* 2007;99:1154-8.
- Neglia D, Michelassi C, Trivieri MG, Sambuceti G, Giorgetti A, Pratali L, Gallopin M, Salvadori P, Sorace O, Carpeggiani C, Poddighe R, L'Abbate A, Parodi O. Prognostic role of myocardial blood flow impairment in idiopathic left ventricular dysfunction. *Circulation* 2002;105:186-93.
- Abdelmoneim SS, Dhoble A, Bernier M, Erwin PJ, Korosoglou G, Senior R, Moir S, Kowatsch I, Xian-Hong S, Muro T, Dawson D, Vogel R, Wei K, West CP, Montori VM, Pellikka PA, Abdel-Kader SS, Mulvagh SL. Quantitative myocardial contrast echocardiography during pharmacological stress for diagnosis of coronary artery disease: a systematic review and meta-analysis of diagnostic accuracy studies. *Eur J Echocardiogr* 2009;10:813-25.
- Gulati A, Ismail TF, Ali A, Hsu LY, Gonçalves C, Ismail NA, et al. Microvascular Dysfunction in Dilated Cardiomyopathy: A Quantitative Stress Perfusion Cardiovascular Magnetic Resonance Study. *JACC Cardiovasc Imaging* 2019;12:1699-708.
- Cortigiani L, Rigo F, Gherardi S, Galderisi M, Bovenzi F, Sicari R. Prognostic meaning of coronary microvascular disease in type 2 diabetes mellitus: a transthoracic Doppler echocardiographic study. *J Am Soc Echocardiogr* 2014;27:742-8.
- Cortigiani L, Rigo F, Sicari R, Gherardi S, Bovenzi F, Picano E. Prognostic correlates of combined coronary flow reserve assessment on left anterior descending and right coronary artery in patients with negative stress echocardiography by wall motion criteria. *Heart* 2009;95:1423-8.
- Ong P, Safdar B, Seitz A, Hubert A, Beltrame JF, Prescott E. Diagnosis of coronary microvascular dysfunction in the clinic. *Cardiovasc Res* 2020;116:841-55.
- Nishi T, Murai T, Ciccarelli G, Shah SV, Kobayashi Y, Derimay F, Waseda K, Moonen A, Hoshino M, Hirohata A, Yong ASC, Ng MKC, Amano T, Barbato E, Kakuta T, Fearon WF. Prognostic Value of Coronary Microvascular Function Measured Immediately After Percutaneous Coronary Intervention in Stable Coronary Artery Disease: An International Multicenter Study. *Circ Cardiovasc Interv* 2019;12:e007889.
- Qi Y, Gu R, Xu J, Kang L, Liu Y, Wang L, Chen J, Zhang J, Wang K. Index of microcirculatory resistance predicts long term cardiac systolic function in patients with STEMI undergoing primary PCI. *BMC Cardiovasc Disord* 2021;21:66.
- Ai H, Feng Y, Gong Y, Zheng B, Jin Q, Zhang HP, Sun F, Li J, Chen Y, Huo Y, Huo Y. Coronary Angiography-Derived Index of Microvascular Resistance. *Front Physiol* 2020;11:605356.
- Mejia-Renteria H, Lee JM, Choi KH, Lee SH, Wang L, Kakuta T, Koo BK, Escaned J. Coronary microcirculation assessment using functional angiography: Development of a wire-free method applicable to conventional coronary angiograms. *Catheter Cardiovasc Interv* 2021;98:1027-37.
- Shin D, Kim J, Choi KH, Dai N, Li Y, Lee SH, Joh HS, Kim HK, Kim SM, Ha SJ, Jang MJ, Park TK, Yang JH, Song YB, Hahn JY, Choi SH, Choe YH, Gwon HC, Lee JM. Functional angiography-derived index of microcirculatory resistance validated with microvascular obstruction in cardiac magnetic resonance after STEMI. *Rev Esp Cardiol (Engl Ed)* 2022;75:786-96.
- Heidenreich PA, Bozkurt B, Aguilar D, Allen LA, Byun JJ, Colvin MM, et al. 2022 AHA/ACC/HFSA Guideline for the Management of Heart Failure: A Report of the American College of Cardiology/American Heart

- Association Joint Committee on Clinical Practice Guidelines. *Circulation* 2022;145:e895-e1032.
17. Chinese Society of Cardiology, Chinese Myocarditis Cardiomyopathy Collaborative Group. Guidelines for the diagnosis and treatment of dilated cardiomyopathy in China. *J Clinical Cardiology* 2018;34:421-34.
  18. Li J, Gong Y, Wang W, Yang Q, Liu B, Lu Y, Xu Y, Huo Y, Yi T, Liu J, Li Y, Xu S, Zhao L, Ali ZA, Huo Y. Accuracy of computational pressure-fluid dynamics applied to coronary angiography to derive fractional flow reserve: FLASH FFR. *Cardiovasc Res* 2020;116:1349-56.
  19. Ciarambino T, Menna G, Sansone G, et al. Cardiomyopathies: An Overview. *Int J Mol Sci* 2021;22:7722.
  20. Morton G, Chiribiri A, Ishida M, Hussain ST, Schuster A, Indermuehle A, Perera D, Knuuti J, Baker S, Hedström E, Schleyer P, O'Doherty M, Barrington S, Nagel E. Quantification of absolute myocardial perfusion in patients with coronary artery disease: comparison between cardiovascular magnetic resonance and positron emission tomography. *J Am Coll Cardiol* 2012;60:1546-55.
  21. Knaapen P, Götte MJ, Paulus WJ, Zwanenburg JJ, Dijkmans PA, Boellaard R, Marcus JT, Twisk JW, Visser CA, van Rossum AC, Lammertsma AA, Visser FC. Does myocardial fibrosis hinder contractile function and perfusion in idiopathic dilated cardiomyopathy? PET and MR imaging study. *Radiology* 2006;240:380-8.
  22. Nakayama M, Yamamuro M, Takashio S, Uemura T, Nakayama N, Hirakawa K, Oda S, Utsunomiya D, Kaikita K, Hokimoto S, Yamashita Y, Morita Y, Kimura K, Tamura K, Tsujita K. Late gadolinium enhancement on cardiac magnetic resonance imaging is associated with coronary endothelial dysfunction in patients with dilated cardiomyopathy. *Heart Vessels* 2018;33:393-402.
  23. Suda A, Takahashi J, Hao K, Kikuchi Y, Shindo T, Ikeda S, Sato K, Sugisawa J, Matsumoto Y, Miyata S, Sakata Y, Shimokawa H. Coronary Functional Abnormalities in Patients With Angina and Nonobstructive Coronary Artery Disease. *J Am Coll Cardiol* 2019;74:2350-60.
  24. De Maria GL, Scarsini R, Shanmuganathan M, Kotronias RA, Terentes-Printzios D, Borlotti A, Langrish JP, Lucking AJ, Choudhury RP, Kharbanda R, Ferreira VM, Channon KM, Garcia-Garcia HM, Banning AP. Angiography-derived index of microcirculatory resistance as a novel, pressure-wire-free tool to assess coronary microcirculation in ST elevation myocardial infarction. *Int J Cardiovasc Imaging* 2020;36:1395-406.
  25. Scarsini R, Shanmuganathan M, Kotronias RA, Terentes-Printzios D, Borlotti A, Langrish JP, Lucking AJ, Ribichini F, Ferreira VM, Channon KM, Garcia-Garcia HM, Banning AP, De Maria GL. Angiography-derived index of microcirculatory resistance (IMR(angio)) as a novel pressure-wire-free tool to assess coronary microvascular dysfunction in acute coronary syndromes and stable coronary artery disease. *Int J Cardiovasc Imaging* 2021;37:1801-13.
  26. Kotronias RA, Terentes-Printzios D, Shanmuganathan M, Marin F, Scarsini R, Bradley-Watson J, Langrish JP, Lucking AJ, Choudhury R, Kharbanda RK, Garcia-Garcia HM, Channon KM, Banning AP, De Maria GL. Long-Term Clinical Outcomes in Patients With an Acute ST-Segment-Elevation Myocardial Infarction Stratified by Angiography-Derived Index of Microcirculatory Resistance. *Front Cardiovasc Med* 2021;8:717114.
  27. Choi KH, Dai N, Li Y, Kim J, Shin D, Lee SH, et al. Functional Coronary Angiography-Derived Index of Microcirculatory Resistance in Patients With ST-Segment Elevation Myocardial Infarction. *JACC Cardiovasc Interv* 2021;14:1670-84.
  28. Schroder J, Michelsen MM, Mygind ND, Suhrs HE, Bove KB, Bechsgaard DF, Aziz A, Gustafsson I, Kastrup J, Prescott E. Coronary flow velocity reserve predicts adverse prognosis in women with angina and no obstructive coronary artery disease: results from the iPOWER study. *Eur Heart J* 2021;42:228-39.
  29. Sara JD, Widmer RJ, Matsuzawa Y, Lennon RJ, Lerman LO, Lerman A. Prevalence of Coronary Microvascular Dysfunction Among Patients With Chest Pain and Nonobstructive Coronary Artery Disease. *JACC Cardiovasc Interv* 2015;8:1445-53.
  30. Abdu FA, Liu L, Mohammed AQ, Yin G, Xu B, Zhang W, Xu S, Lv X, Fan R, Feng C, Shi T, Huo Y, Xu Y, Che W. Prognostic impact of coronary microvascular dysfunction in patients with myocardial infarction with non-obstructive coronary arteries. *Eur J Intern Med* 2021;92:79-85.
  31. Melikian N, Vercauteren S, Fearon WF, Cuisset T, MacCarthy PA, Davidavicius G, Aarnoudse W, Bartunek J, Vanderheyden M, Wyffels E, Wijns W, Heyndrickx GR, Pijls NH, de Bruyne B. Quantitative assessment of coronary microvascular function in patients with and without epicardial atherosclerosis. *EuroIntervention* 2010;5:939-45.
  32. Luo C, Long M, Hu X, Huang Z, Hu C, Gao X, Du Z. Thermodilution-derived coronary microvascular resistance and flow reserve in patients with cardiac syndrome X. *Circ Cardiovasc Interv* 2014;7:43-8.

33. Liu M, Wang F, Wang Y, Jin R. Atorvastatin improves endothelial function and cardiac performance in patients with dilated cardiomyopathy: the role of inflammation. *Cardiovasc Drugs Ther* 2009;23:369-76.
34. Fu L, Shang X, Zhang X. The Impact of Atorvastatin on Cardiac Performance for Dilated Cardiomyopathy: A Meta-analysis of Randomized Controlled Studies. *Heart Surg Forum* 2020;23:E329-34.
35. Sayed N, Liu C, Ameen M, Himmati F, Zhang JZ, Khanamiri S, Moonen JR, Wnorowski A, Cheng L, Rhee JW, Gaddam S, Wang KC, Sallam K, Boyd JH, Woo YJ, Rabinovitch M, Wu JC. Clinical trial in a dish using iPSCs shows lovastatin improves endothelial dysfunction and cellular cross-talk in LMNA cardiomyopathy. *Sci Transl Med* 2020.
36. Bairey Merz CN, Pepine CJ, Shimokawa H, Berry C. Treatment of coronary microvascular dysfunction. *Cardiovasc Res* 2020;116:856-70.
37. Pearson JT, Thambyah HP, Waddingham MT, Inagaki T, Sukumaran V, Ngo JP, Ow CPC, Sonobe T, Chen YC, Edgley AJ, Fujii Y, Du CK, Zhan DY, Umetani K, Kelly DJ, Tsuchimochi H, Shirai M. -blockade prevents coronary macro- and microvascular dysfunction induced by a high salt diet and insulin resistance in the Goto-Kakizaki rat. *Clin Sci (Lond)* 2021;135:327-46.
38. Matta A, Nader V, Galinier M, Roncalli J. Transplantation of CD34+ cells for myocardial ischemia. *World J Transplant* 2021;11:138-46.
39. Diaz-Navarro R, Urrútia G, Cleland JG, Poloni D, Villagran F, Acosta-Dighero R, Bangdiwala SI, Rada G, Madrid E. Stem cell therapy for dilated cardiomyopathy. *Cochrane Database Syst Rev* 2021;7:CD013433.
40. Movsesian MA, Alharethi R. Inhibitors of cyclic nucleotide phosphodiesterase PDE3 as adjunct therapy for dilated cardiomyopathy. *Expert Opin Investig Drugs* 2002;11:1529-36.
41. Woitek F, Zentilin L, Hoffman NE, Powers JC, Ottiger I, Parikh S, et al. Intracoronary Cytoprotective Gene Therapy: A Study of VEGF-B167 in a Pre-Clinical Animal Model of Dilated Cardiomyopathy. *J Am Coll Cardiol* 2015;66:139-53.
42. Li M, Su H, Jiang M, Zuo Z, Su Z, Hao L, Yang J, Zhang Z, Wang H, Kong X. Predictive value of thrombolysis in myocardial infarction frame count for coronary microvascular dysfunction evaluated with an angiography-derived index of microcirculatory resistance in patients with coronary slow flow. *Quant Imaging Med Surg* 2022;12:4942-52.
43. Borra D, Andalò A, Paci M, Fabbri C, Corsi C. A fully automated left atrium segmentation approach from late gadolinium enhanced magnetic resonance imaging based on a convolutional neural network. *Quant Imaging Med Surg* 2020;10:1894-907.

**Cite this article as:** Li M, Su H, Zuo Z, Zhang Z, Li M, Su F, Yao W, He Y, Kong X, Wang H. The role of the angiography-derived index of microcirculatory resistance in the prognosis of patients with dilated cardiomyopathy. *Quant Imaging Med Surg* 2023;13(4):2647-2659. doi: 10.21037/qims-22-1060

Supplementary

	LAD-caIMR $\leq$ 29.8 (n=70)	LAD-caIMR >29.8 (n=25)	P value
Composite end points	13 (18.6)	23 (92.0)	<0.001
HF-rehospitalization	1 (1.4)	21 (84.0)	<0.001
Device implantation	6 (9.2)	0 (0.0)	0.335
Heart transplantation	1 (1.5)	0 (0.0)	1.000
Death	5 (7.1)	2 (8.0)	1.000
	LCX-caIMR $\leq$ 25.5 (n=47)	LCX-caIMR >25.5 (n=48)	
Composite end points	9 (19.1)	27 (56.3)	<0.001
HF-rehospitalization	3 (6.4)	19 (39.6)	<0.001
Device implantation	3 (6.4)	3 (6.3)	1.000
Heart transplantation	0 (0.0)	1 (2.1)	1.000
Death	3 (6.4)	4 (8.3)	1.000
	RCA-caIMR $\leq$ 29.7 (n=62)	RCA-caIMR >29.7 (n=33)	
Composite end points	14 (22.6)	22 (66.7)	<0.001
HF-rehospitalization	7 (11.3)	15 (45.5)	<0.001
Device implantation	4 (6.5)	2 (6.1)	1.000
Heart transplantation	0 (0.0)	1 (3.0)	0.347
Death	4 (6.5)	3 (9.1)	0.691

**Figure S1** Clinical outcome stratified by the caIMR of 3 coronary arteries. HF, heart failure; LCX-caIMR, coronary angiographic index of microcirculatory resistance for left circumflex artery; RCA-caIMR, coronary angiographic index of microcirculatory resistance for right coronary artery.